MNRAS **000**, 1–7 (2017) Preprint 6 July 2017 Compiled using MNRAS LATEX style file v3.0

Influence of reduced light speed approximation on reionization fronts speed in cosmological RHD simulations

Nicolas Deparis[1]★, Dominique Aubert[1], Pierre Ocvirk[1]
[1] *Observatoire Astronomique de Strasbourg, CNRS UMR 7550, Universite de Strasbourg, Strasbourg,France*

Accepted XXX. Received YYY; in original form ZZZ

ABSTRACT
We run a set of radiative hydrodynamic cosmological simulations of reionization to explore the link between the ionization rate and the reduced speed of light approximation. We introduce a method to compute the ionization front speed based on the reionization redshift map a posteriori. We found that for a reduced speed of light greater than $\tilde{c} = 0.05$, the front speed is limited only at the end of the reionization. In the case of lower reduced speed of light, the RSLA imply a limited fronts speed during the whole reionization process.

Key words: cosmology: dark ages, reionization, first stars - methods: numerical

1 INTRODUCTION

A central process to consider when simulating the Epoch of Reionization (EoR) is the light propagation through the Universe. As light is several order faster than hydrodynamical processes generally considered in cosmological simulations, introducing radiative transfer (RT) can be computationally challenging.

There is two main families of RT codes in EoR simulations:

- Ray tracing/Monte Carlo methods consider light as group of photons (eg. CRASH Maselli et al. (2003), C^2-RAY Mellema et al. (2006)). Each sources launch a given number of photons, in straight line and randomized direction.
- Moment based methods consider light as a fluid (eg. OTVET Gnedin & Abel (2001a), ATON Aubert & Teyssier (2008)). Each source act as a fountain where light flows out.

Ray tracing technique can be very accurate as it is closer to the physical behaviour of light. The main drawback of this accuracy is that the computational cost of these techniques is directly linked to the number of sources. At the opposite, the moment base method can be a bit more inaccurate on certain physical effects (eg. the shadowing effect by dense clump) but is independent of the number of sources. This study is limited to the case where the radiative transfer solver use a moment based description and more specifically the 'M1 closure model' for the Eddington tensor implemented in EMMA (Aubert et al. 2015).

Some ray-tracing technique use infinite speed of light, but in the vast majority of case in cosmological simulations, light speed is finite (ie consider temporal evolution of light). The main constraint for time dependent RT code is due to the Courant-Friedrichs-Lewy (CFL) condition. It impose that the higher the velocity of a process is, the higher the temporal resolution has to be to accurately simulate its propagation. The time step Δt is computed using:

$$\Delta t = C_{CFL} \cdot \frac{\Delta x}{v}, \tag{1}$$

where $C_{CFL} < 1$, Δx is the spatial resolution and v is the speed of the considered process.

As light has the highest known velocity, it needs a small Δt and so a large amount of timestep to follow its propagation on a given period. In the aims to reduce this cost, two methodologies has emerged. The first one consist into taking profit of the recent hardware evolution, due to their highly parallele capability, using Graphical Processing Unit (GPU) can divide the computational time by almost two orders of magnitude. The second method is the one we are looking at in this study, the reduced speed of light approximation (RSLA) (Gnedin & Abel 2001b; Aubert & Teyssier 2008). The main idea of this technique is that standard hydrodynamic cosmological simulation use the Newtonian approximation, ie the speed of considered physical process (DM and gas) is several orders of magnitude lower than the physical speed of light. So as the light speed is significantly higher than others considered process, lowering its velocity in the simulation should not have a significant impact on the results, while at the same time allowing a comfortable gain on the computational cost.

The RSLA consider that the light evolve at a fraction

★ E-mail: nicolas.deparis@astro.unistra.fr

of its real speed:

$$v = \tilde{c} \cdot c, \tag{2}$$

where c is the physical light speed and $\tilde{c} \leq 1$ is the RSLA factor.

In a case where the reionization history stays the same between $\tilde{c} = 1$ and $\tilde{c} = 0.1$, we could gain a factor ten in the computation of radiative processes, which is really appreciable as radiation represents approximately half of the computational cost in this kind of simulation when $\tilde{c} = 1$.

In this study, we explore how reducing the speed of light in the simulation, influence the evolution of ionization fronts during the reionization epoch.

We present a set of RHD simulations with different RSLA and observe that even if the photon budget stays the same between runs, the reionization occurs at different time and that the delay is correlated with the RSLA. We introduce a method to compute the reionization front speed using reionization redshift maps. From this ionization speed maps, we observe the the reionization is a two stages process. In a first part, the reionization rate as well as the fronts speed stay pretty constant through time, and in a second part fronts reach the voids and reionization is accelerated. We show that the RSLA mostly limits the reionization in the acceleration phase, but that for $\tilde{c} > 0.05$ the constant speed phase is almost not impacted. In the case of $\tilde{c} < 0.05$, the fronts speed are limited during the whole reionization process.

2 METHODOLOGY

Simulations are runs with `EMMA` an AMR cosmological code with fully coupled radiative hydrodynamic (Aubert et al. 2015). The light is considered as a fluid, its propagation is followed by a HLL Riemann solver coupled with the M1 approximation (Levermore 1984; González et al. 2007; Aubert & Teyssier 2008).

We run a set of simulations at a similar resolution of production runs like eg CODA (Ocvirk et al. 2015) or CROC (Gnedin 2014) but with smaller volume. We are considering $\left(8h^{-1}\mathrm{cMpc}\right)^3$ volume, simulated from redshift z=150 to the end of the reionization ($5 < z < 6$). Dark matter is resolved with 256^3 particles with a mass of $3.4 \cdot 10^6 M_\odot$. Hydrodynamics and radiation are simulated on a grid 256^3 resolution elements for a coarsest spatial resolution of 46 ckpc. The grid is refined according to a semi-Lagrangian scheme and the refinement is not allowed if the spatial resolution of the newly formed cells is under 500pc. Our stellar mass resolution is set to be equal to $7.2 \cdot 10^4 M_\odot$. We calibrate our emissivity model using Starburst99, with a population of $10^6 M_\odot$ having a Top-Heavy initial mass function and a Z=0.001 metalicity. To limit the number of unknowns, we do not consider supernovae feedback here.

All simulations are run with the exact same parameters and initial conditions, except for $\tilde{c}$, the ratio between the simulated speed of light over the real light speed. We run a set of six simulations with $\tilde{c} = 1$, $\tilde{c} = 0.3$,$\tilde{c} = 0.1$, $\tilde{c} = 0.05$, $\tilde{c} = 0.02$ and $\tilde{c} = 0.01$. Star formation is calibrated with Bouwens et al. (2015), and the emissivity of radiative sources on Fan et al. (2006), using the c=0.02 run.

3 RESULTS

3.1 Cosmic star formation and ionization histories

Fig 1a presents the cosmic star formation histories (SFH) as a function of the RSLA. This measure shows that the RSLA does not change the cosmic SFH. And as ionizing photons are emitted by newly formed stars, the photons budget is not impacted of the RSLA.

Fig 1b presents the average volume weighted ionization state as a function of time $X_V(t)$:

$$X_V(t) = \frac{\int x_{(t)} \cdot dV}{\int dV}, \tag{3}$$

with the local ionization fraction :

$$x_{(t)} = \frac{n_{H+}}{n_H} \tag{4}$$

We observe a direct link between the ionization history and the RSLA. The slower the light is, the later the reionization occurs.

We define the reionization redshift as the redshift where the volume weighted hydrogen neutral fraction pass below $X_V = 10^{-4}$. Fig 1c presents obtains reionization redshift as a function of the reduced speed of light.

Reionization redshift converges as $\tilde{c}$ is close to 1, There is a priori no reason for reionization redshift to converge with $\tilde{c} = 0.1$, but this observation may be a point in favour of infinite speed of light techniques.

At the opposite, reionization redshift rapidly decline with $\tilde{c}$. For instance, $\tilde{c} = 0.1$ presents a delay of ≈ 60 Myr and less than 0.5 in redshift but these values are extended to ≈ 425 Myr and almost 2.2 in redshift for the $\tilde{c} = 0.01$ run.

Using Fig 1a, we conclude that the delay observed in the reionization time is not due to a change in the ionizing energy budget by radiative feedback.

It is plausible that the faster the light is, the sooner the photon could reach the under-dense regions, and then the sooner the reionization. The fact is that the reionization fronts do not evolve at light speed, If the ionization fronts evolve at a negligible speed compared to the speed of light, it is possible that changing the speed of light does not affect front speed. However this is not what we observe and fronts speed has to be non negligible compared to speed of light.

3.2 Average ionization rate

From previous section we observe that with the same SFR, the ionization history change with the RSLA, so the capacity of stars to reionize their environment is evolving with the light speed. In this section we quantify this effect by introducing a stellar mass weighted average ionization rate.

First we define de the average ionization rate $\dot{X}_{(t)}$ as the temporal derivative of the ionization history.

$$\dot{X}_{(t)} = \frac{\partial X_{(t)}}{\partial t} = \left[\mathrm{yr}^{-1}\right]. \tag{5}$$

By dividing the average ionization rate $\dot{X}_{(t)}$ by the average star formation rate $\dot{\rho}^*_{(t)}$ in $\left[M_\odot \cdot yr^{-1} \cdot ckpc^{-3}\right]$, we

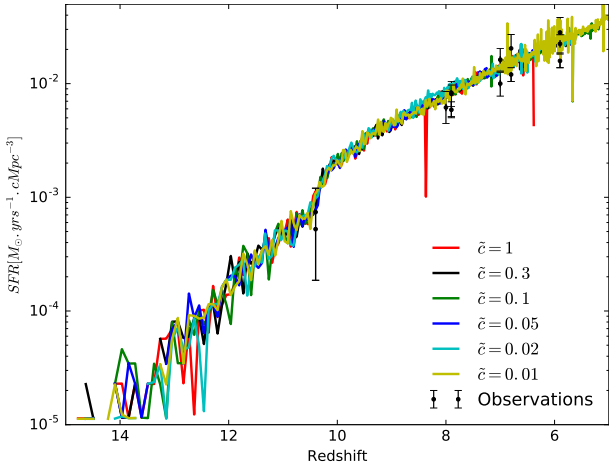

(a)

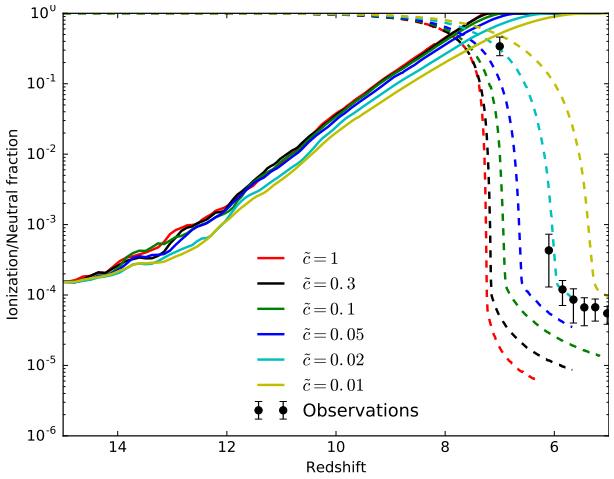

(b)

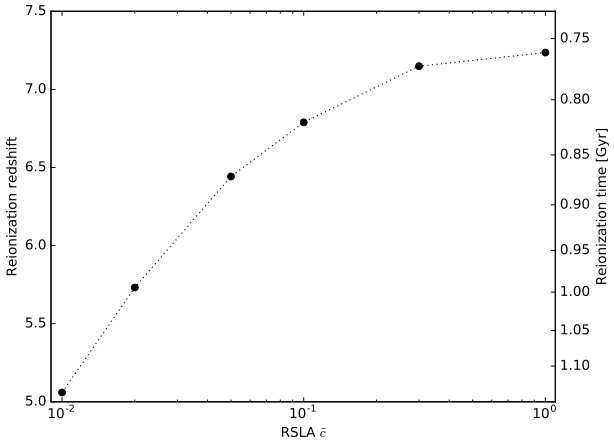

(c)

Figure 1. (a) Cosmic star formation histories; (b) volume weighted ionization (solid lines) and neutral (dashed lines) fraction function of redshift for different reduced speed of light. The RSLA get almost no impact on the cosmic SFR but significantly change ionization histories. (c) Reionization redshift function of RSLA. Reionization occurs later when the numerical speed of light is slower.

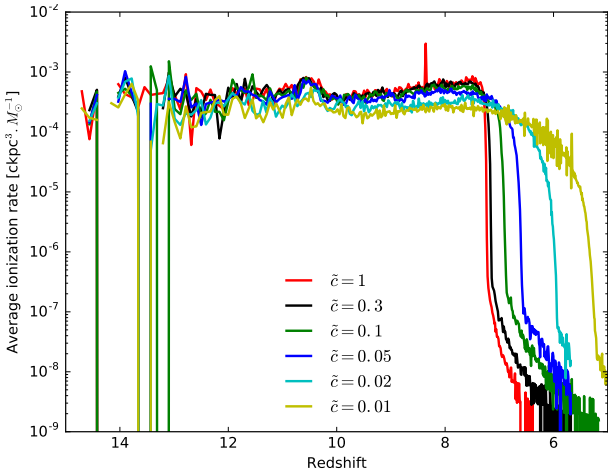

Figure 2. Stellar mass weighted average ionization rate as a function of redshift for different reduce speed of light.

quantify the ability of newly formed stars to ionize their environment :

$$\dot{X}_{(\dot{\rho}^*)} = \frac{\dot{X}_{(t)}}{\dot{\rho}^*_{(t)}} \left[\text{ckpc}^3 \cdot \text{M}_\odot^{-1}\right]. \quad (6)$$

It represents the amount of volume each solar masses of stars, newly formed in the simulation, will reionized. The resulting stellar mass weighted ionization rate computation is presented on Fig. 2 as a function of redshift and RSLA. Each run get an almost flat ionization rate before redshift z=8. In this phase the ionization rate is governed by the star formation and tends to be independent of the RSLA for runs with $\tilde{c} \geq 0.05$, but is lowered for $\tilde{c} < 0.05$.

During this flat phase, the average ionization rate before z=8 are going from $5.1 \cdot 10^{-4}$ ckpc^3.$M_\odot^{-1}$ for the $\tilde{c} = 1$ run, to $2.4 \cdot 10^{-4}$ ckpc^3.$M_\odot^{-1}$ for the $\tilde{c} = 0.01$ run.

The main difference comes in a second time for redshift $z < 8$, where light start reaching under-dense regions and ionized bubbles start to merge. It then become more difficult for the radiation emitted by newly formed stars to ionize neutral medium as the neutral gas is rarer. This transition happens almost instantaneously with $\tilde{c} = 1$ and become slower with smaller light speeds.

3.3 Ionization maps

Ionization redshift maps offers a good tool to analyse the whole reionization process using a single data field. Redshift maps are obtained by keeping in memory, for each cell, the time when its ionization fraction pass a given threshold. The computation is done during simulation runtime to get the highest temporal resolution possible.

It is possible to choose to keep the first or the last reionization time. The difference between first and last ionization maps will be significant in dense regions where recombination can be high but will globally be the same in under-dense region that do not recombine. As under-dense regions represent the major part of the volume, the volume weighted ionization state is mostly governed by them. In this study, the cell reionization time is considered to be the first time

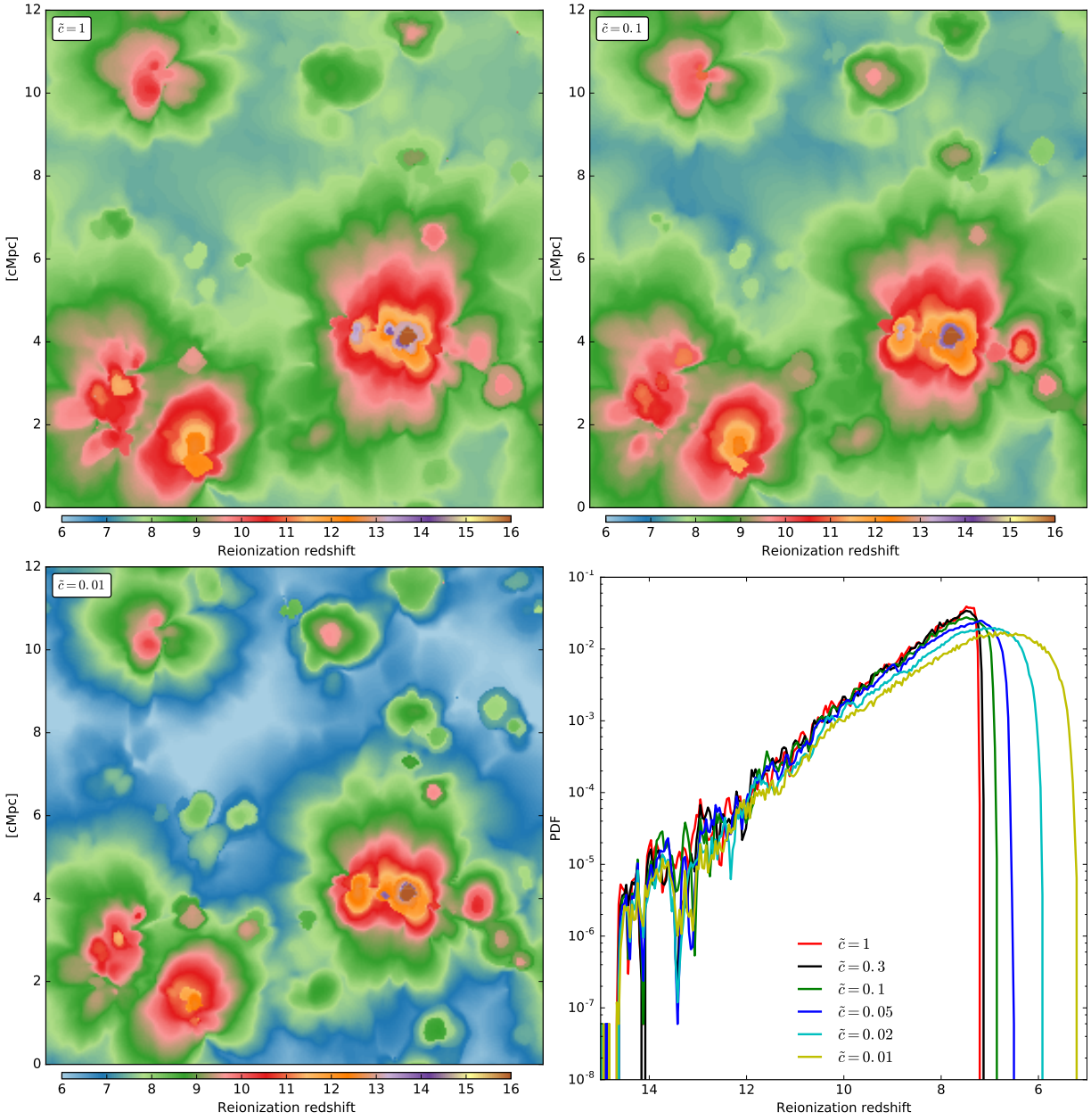

Figure 3. Maps and PDF of reionization redshift for runs with different reduced speed of light.

when the volume weighted ionization fraction passes through 50%.

Fig. 3 shows three maps of reionization redshift for three RSLA, and the reionization redshift probability density function (PDF) for all runs.

Maps are one coarse cells (46 ckpc) thick slices taken at the same coordinate in the z axis for the tree simulations. The slice is chosen to contain the first cell to pass the ionization threshold in the $\tilde{c} = 0.1$ simulation.

We observe a similar global behaviour between runs. The sources are located at the same place independently of the run, which is coherent with the fact that the ionizing feedback do not significantly change global star formation processes in our simulation (Fig 1a). Radiation escapes high density regions in comparable butterfly shapes.

The $\tilde{c} = 0.1$ run is quite similar to the the $\tilde{c} = 1$. Dark green isocontours ($z \approx 6$) are located at the same place and have the same shape. The main difference between these runs appears at low redshift when the light reach the voids (blue shades). Voids reionize a bit slower at $\tilde{c} = 0.1$ than at $\tilde{c} = 1$ due to the time taken by light to reach them. The behaviour is even more pronounced for $\tilde{c} = 0.01$ where the voids reionization is clearly late compared to faster reduced speed of light(apparition of blue regions).

This is particularly clear regarding to the redshift PDF, at high redshift all PDF are similar, but the difference slowly increase with time, and the cumulative effect leads to a significant delay on the global reionization. This is in accordance with the observations made on the volume weighted ionization history (Fig. 1b), as the voids represent the major

part of the volume, runs with faster light reionize faster, due to the ability of light to reach voids sooner.

3.4 Ionization fronts speeds

The reionization maps represent a time at each point of the space. Considering the spatial gradient of this map, we obtain the information of the time needed to reionize each cells.

Due to the expansion, the grid is evolving through time. The size of each cells depends of its reionization time, and as we want to follow a physical process we want it in physical units and not in comoving units. The gradient of a cell i is weighted by a^i the scale factor of the cell at its reionization time.

We use a discrete gradient with the form:

$$\vec{\nabla} t^i_{reio} \approx \frac{t^{i+1} - t^{i-1}}{2a^i \left(x^{i+1} - x^{i-1}\right)}. \quad (7)$$

This gradient represents the time needed to ionize a given distance (eg in [yr.pc^{-1}]), the reverse of this gradient is analogue to a velocity (eg in [pc.yr^{-1}]) :

$$V_{reio} = \frac{1}{\left|\vec{\nabla} t_{reio}\right|}. \quad (8)$$

V_{reio} can be interpret as an estimator to the speed of the reionization front passing through the cell.

Fig. 4 shows maps of reionization front speed obtained with this method for three runs with different reduced speed of light.

Reionization speed can be greater than the speed of light in the simulation, up to several time. The limit case is when two neighbouring cells reionize at the same timestep, their gradient became null and the associated reionization speed became infinite. This can happen in two cases:

- In over-dense regions, where two adjacent cells have simultaneous star forming events.
- In under-dense regions, during the collapse of two ionization fronts.

This part of spurious speeds represents a small fraction of the volume (with a fraction of $8 \cdot 10^{-5}$ in the worst case).

On the PDF, we observe that limited light speed, do not avoid the presence of front speed over its value. There is still front speed of 10^{-1} when $\tilde{c} = 10^{-2}$ but the probability to find such a speed in the volume is significantly reduced.

The concentric alternation between high and low speeds fronts is induced by the consecutive events of star formation. Reionization fronts can only expand if there are internal radiative sources, but star formation is not continuous and appends by burst. So fronts stop their progress during the time between two consecutive star formation events.

The number of these concentric pattern decrease with the speed of light, With the $\tilde{c} = 0.01$ run the map is lot smoother than the $\tilde{c} = 1$ run.

We found an average and most probable front speed going from respectively $\approx$ 2400km.s^{-1} and $\approx$ 1400km.s^{-1} for the $\tilde{c} = 1$ run to $\approx$ 1000km.s^{-1} and $\approx$ 800km.s^{-1} for the $\tilde{c} = 0.01$ run.

3.5 Speed of ionization fronts as a function of redshift

We show in the last section that reducing the speed of light in the simulation limit the probability to find a front speed above this limit. In the two previous section we have associated a redshift and a speed at each point of space. In this section we analyse the evolution of the reionization front speed as a function of redshift.

Fig. 5 presents the distributions of fronts speed as a function of redshift, as well as the evolution of the average fronts speed for different RSLA.

In the $\tilde{c} = 1$ run, we observe that for z>8, the distributions of speeds are always between $\approx 10^{-1}$ and $\approx 10^{-4}$. This phase is then followed by a quick acceleration peak, We observe a two times process, in a first time, light escape over-dense regions at an average constant speed and in a second time the percolation of ionized bubble allow the light to reach under-dense regions. In this regions, the fronts speeds are not limited by the interaction with baryons. The light is free to fill the voids and fronts speeds are able to reach the real speed of light. After the reionization, where ionization bubbles has collapse, the probability to find an high speed front drop suddenly, as the whole volume is ionized.

In the $\tilde{c} = 0.1$ run, the first phase is not impacted by the RSLA: even with $\tilde{c} = 1$ the front speeds where already lower than $\approx 10^{-1}$. The main difference appears in the second phase: the $z < 8$ peak is significantly reduced by the RSLA. With $\tilde{c} = 1$ the fronts where able to reach speeds greater than 0.1c, by setting $\tilde{c} = 0.1$ velocities of this fronts are limited to $\approx 0.1c$. As the fronts speeds can be as high as in the $\tilde{c} = 1$ run, the end of the reionization is slightly delayed.

In the $\tilde{c} = 0.01$ run, the propagation of light is already limited at the beginning of the reionization. In the two previous runs, a part of the fronts speeds where already greater than $\approx 0.01c$ since the beginning of the reionization. This leads to an important cumulative delay in the reionization redshift. Moreover, the final peak is almost totally smoothed.

On the averaged plot, we clearly observe this almost constant front speed followed by an acceleration for redshift $z < 8$. In the $z > 8$ constant phase, the average front speed goes from $4.1 \cdot 10^{-3}[c]$ for the $\tilde{c} = 1$ run to $2.2 \cdot 10^{-3}[c]$ for the $\tilde{c} = 0.01$ run. This constant phase is the same that we observe on Fig. 2, the ionization rate is constant when the fronts speed are constants. In the constant phase, all runs with RSLA higher than 0.05 have a similar average speed and ionization rate. But for RSLA lower than 0.05 both are limited from the beginning of the reionization. This link between ionization rate and front speed is also visible on Fig. 3, the PDF of reionization redshift sensitively the same for redshift $z > 8$ if $\tilde{c} > 0.05$, but presents a shift starting at redshift $z \approx 14$ for $\tilde{c} < 0.05$.

The acceleration for redshift $z < 8$ is significantly impacted by the RSLA. With an large speed of light the box flashes faster at the end of the reionization than with lower value. This final acceleration correspond to the light reaching under dense region and in all cases the average front speed is limited by the RSLA.

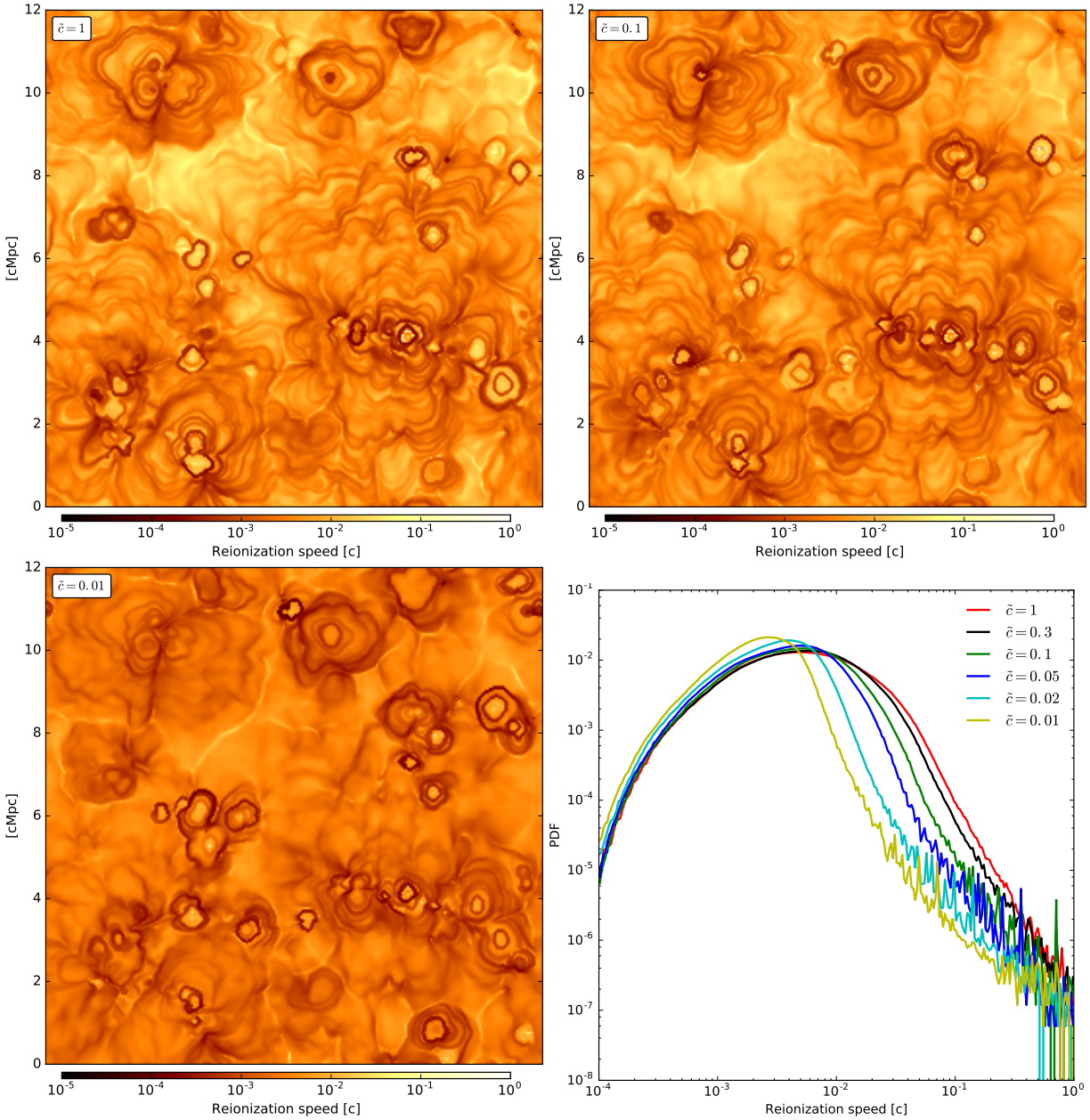

Figure 4. Maps and PDF of reionization front speed for runs with different reduced speed of light approximations. Front speed are expressed relatively to the real speed of light.

4 DISCUSSIONS AND CONCLUSION

We present a method to compute ionization front speed a posteriori using reionization maps. With this method we found that reducing the speed of light in the simulation tends to limit the ionization front speed.

Analysing the average front speed as a function of redshift, we observe that the reionization append in two phases. First a constant speed phase, followed by a acceleration phase.

During the constant phase, the average value do not depends of $\tilde{c}$ for $\tilde{c} > 0.05$. In all case, the acceleration phase is strongly impacted by the choice of the RSLA.

Observations from Fan et al. (2006) impose time constraints for the very end of the reionization. But we show that the RSLA can significantly impact the speed of the reionization especially at the end of it. Its seems then difficult to conciliate RSLA with a well timed reionization by obsevationnal constraints. However the growth of ionized bubbles can be accurately studied even with $\tilde{c}$ down to 5%.

In conclusion, the RSLA can be a good approximation down to $\tilde{c}$ = 0.05, if the goal is to analyse dense region behaviour. Things are more complicated while considering the ionization of cosmic voids, as in those ones the front speed can be as high a c, the RSLA is always a limitating factor.

The fact that front speed are mostly impacted in the voids tends to comfort us in the validity of halo centric studies using the RSLA. As this studies are focused on dense region, fronts speeds are well resolved in this phase.

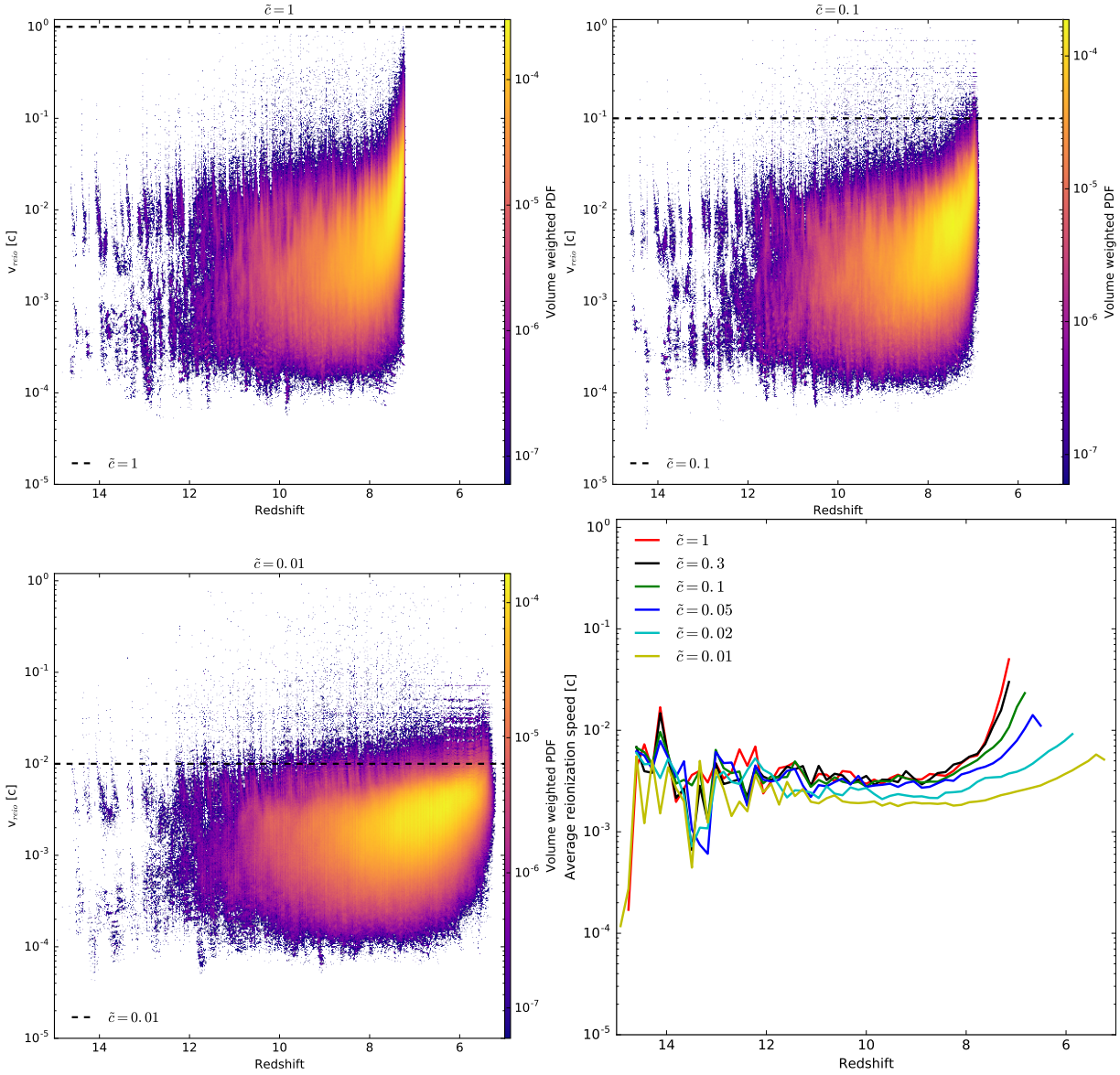

Figure 5. 2D histogram and average of reionization speed in unit of the real speed of light as a function of redshift for different RSLA. The horizontal dashed line represents $\tilde{c}$ the light speed in the simulation.

ACKNOWLEDGEMENTS

This work is supported by the ANR ORAGE grant ANR-14-CE33-0016 of the French Agence Nationale de la Recherche.

REFERENCES

Aubert D., Teyssier R., 2008, Monthly Notices of the Royal Astronomical Society, 387, 295
Aubert D., Deparis N., Ocvirk P., 2015, Monthly Notices of the Royal Astronomical Society, 454, 1012
Bouwens R. J., et al., 2015, The Astrophysical Journal, 803, 34
Fan X., Carilli C. L., Keating B., 2006, Annual Review of Astronomy and Astrophysics, 44, 415
Gnedin N. Y., 2014, arXiv:1403.4245 [astro-ph]
Gnedin N. Y., Abel T., 2001a, New Astron., 6, 437
Gnedin N. Y., Abel T., 2001b, New Astronomy, 6, 437
González M., Audit E., Huynh P., 2007, A&A, 464, 429
Levermore C. D., 1984, J. Quant. Spectrosc. Radiative Transfer, 31, 149
Maselli A., Ferrara A., Ciardi B., 2003, MNRAS, 345, 379
Mellema G., Iliev I. T., Alvarez M. A., Shapiro P. R., 2006, New Astron., 11, 374
Ocvirk P., et al., 2015, preprint, 1511, 11
Semelin B., Combes F., Baek S., 2007, A&A, 474, 365

This paper has been typeset from a TEX/LATEX file prepared by the author.